X-ray Photoelectron Spectroscopy and X-ray Emission Spectroscopy of Poly(ethylene oxide) and Poly(vinyl alcohol): Experiment and Theory

P. Boulanger,† C. Magermans,† J. J. Verbist,*,† J. Delhalle,‡ and D. S. Urch§

Laboratoire Interdisciplinaire de Spectroscopie Electronique and Laboratoire de Chimie Théorique Appliquée, Département de Chimie, Facultés Universitaires Notre-Dame de la Paix, 61, rue de Bruxelles, B-5000 Namur, Belgium, and Department of Chemistry, Queen Mary College, University of London, Mile End Road, London E1 4NS, Great Britain

Received April 24, 1990; Revised Manuscript Received October 9, 1990

ABSTRACT: X-ray emission spectroscopy (XES) and X-ray photoelectron spectroscopy (XPS) measurements of valence band spectra of poly(ethylene oxide) (POE) and poly(vinyl alcohol) (PVOH) are reported. With the help of ab initio quantum chemistry calculations, some of the observed differences in line intensities and position are interpreted in terms of configurational differences in the polymeric units.

1. Introduction

The elaboration of polymer films on various substrates (metals, glasses, etc.) modifies their surface properties and often leads to new materials with potential applications in highly demanding fields (electronics, catalysis, biotechnology, space). There are various ways of producing such films: electrochemistry, Langmuir–Blodgett deposition, spin coating, chemical vapor deposition, etc. The resulting films are usually very thin and strongly adherent so that it is often impossible to investigate their composition, nature, and molecular structure by classical techniques such as IR and NMR spectroscopies. It is therefore necessary to use analytical methods adapted to surface studies, which unfortunately yield information difficult to interpret.

As demonstrated in 1974 by quantum mechanical simulations, valence XPS (X-ray photoelectron spectroscopy) spectra can provide information on the primary and secondary structures of organic polymers.[1] A few comparisons[2,3] between theoretically simulated and measured valence band spectra of pure hydrocarbon polymers have provided a preliminary basis for establishing relationships between XPS valence features and the polymer geometrical structure. Recently, Boulanger et al.[4] have made a detailed experimental and theoretical study of the valence XPS spectra of hexagonal and orthorhombic poly(oxymethylenes) whose chains are characterized by different dihedral angles around the C–O bonds. The overall agreement so far noted between experimental and theoretically simulated spectra provides support and motivation for proceeding further along these lines.

There is also an obvious interest in finding other techniques that could be applied in the particular case of thin polymer films and from which complementary information on the primary and secondary structures of the polymers could be deduced. One such technique, which has so far been left unexploited in polymer structure analysis, is X-ray emission spectroscopy (XES). In this work XES spectra of polymer systems are recorded to study their valence electronic structure and compare the results with those of XPS measurements obtained on the same samples. The systems chosen in this first application of XES in connection with valence band electronic structure studies of polymers are poly(ethylene oxide), $-[CH_2CH_2O]-_n$ (POE), and poly(vinyl alcohol), $-[CH_2-CH(OH)]-_n$ (PVOH). They only differ by the position of the oxygen atom relative to the carbon atoms in the monomeric unit (structural isomerism). In POE, the oxygen atom is linked to two carbon atoms and thus included in the polymer backbone; in PVOH the oxygen atom is part of the hydroxyl pendant group grafted to a purely hydrocarbon chain. Our aim is to compare the XES spectra and the valence XPS data with the corresponding theoretical simulations on model compounds. The principles of the spectroscopic and theoretical techniques used in this paper are briefly discussed in sections 2 and 3, respectively. The experimental conditions of the work are detailed in section 4, and the results are discussed in section 5.

2. XPS and XES Spectroscopies

Since, to our knowledge, the reported XES measurements on polymers[5] have essentially been carried out to assess the performances of soft X-ray detectors, we felt it was appropriate to briefly describe the basics of both XPS and XES spectroscopies and underscore their differences and complementarities.

X-ray Photoelectron Spectroscopy (XPS).[6] By irradiation of a gas sample with X-ray monochromatic radiation, the resulting perturbation induces, with a specific probability, the ejection of core and/or valence photoelectrons (Figure 1). The process can be sketched as

$$M_0 + h\nu \rightarrow M_i^+ + e^- \quad (1)$$

where M_0 represents the isolated neutral system (molecule, oligomer, or polymer) in its ground state (0), M_i^+ represents the positive ion (+) of the system in the excited final state i, e^- is the emitted photoelectron carrying a kinetic energy E_k, and $h\nu$ is the ionizing photon energy. From the energy balance, $E_0 + h\nu = E_i^+ + E_k$, corresponding to (1), one can define the binding energy, E_b, which in the gas-phase case is equal to the ionization energy, I_i:

$$E_b = h\nu - E_k = E_i^+ - E_0 = I_i \quad (2)$$

In the case of a solid sample, the binding energy is referenced with respect to the Fermi level, E_F, and the ionization energy is determined to within a constant ϕ, called the work function of the solid. E_b' is the energy

† Laboratoire Interdisciplinaire de Spectroscopie Electronique, Facultés Universitaires Notre-Dame de la Paix.
‡ Laboratoire de Chimie Théorique Appliquée, Facultés Universitaires Notre-Dame de la Paix.
§ University of London.

0024-9297/91/2224-2757$02.50/0

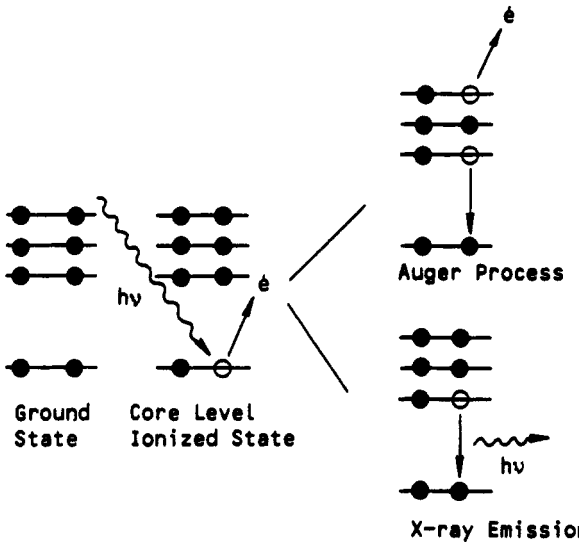

Figure 1. Schematic view of the photoelectronic effect and consecutive processes of relaxation.

required to raise the electron to the Fermi level.

$$I_i = E_b' + \phi \tag{3}$$

Roughly speaking, a photoelectron spectrum provides an experimentally based description of the electronic structure of the compound since the spectral lines correspond to the difference in total energies, $E_i^+ - E_0$, of the various excited final states Ψ_i^+ of the ion (M_i^+) and the ground state Ψ_0 of the neutral system (M_0). The lines have an intensity corresponding to the photoionization cross-section $\Sigma_{0,i}$ proportional to the square of the modulus of the integral

$$\Sigma_{0,i} \propto |\int \Psi_0 P \Psi_i^+ \, d\tau|^2 \tag{4}$$

where P is the associated transition operator.

An accurate calculation of the energy lines and their intensities is a formidable task that is only possible for simple systems. Thus, interpretations are most often based on results of one-electron models, mostly LCAO–MO ab initio Hartree–Fock, and rely on the assumed validity of the frozen orbital model (Koopmans' theorem[7]). In this approximate description, one associates the main peaks of the photoelectron spectrum to the one-electron orbital energies ϵ_i of the neutral system. Due to an approximate cancellation of two opposing effects (orbital relaxation and electronic correlation), this approximation often predicts the right sequence of the highest energy (valence) levels. However, one should remain cautious because the use of Koopmans' theorem leads often to quantitative and sometimes qualitative discrepancies.

In the LCAO–MO framework, a useful approximation for the intensities is to use the electric dipole approximation as the transition operator P between the LCAO expansion of the orbitals φ_i of the neutral system and a plane wave Ψ_k representing the wave function of the photoemitted electron (a typical value of the wavelength λ is 0.32 Å). Then, (4) becomes

$$\Sigma_{0,i} \approx \sigma_i \propto |\int \{\sum_a \sum_{p(a)} C_{ip(a)} \chi_{p(a)}(\mathbf{r})\}(e\mathbf{r}) \Psi_k(\mathbf{r}) \, d\tau|^2 \tag{5}$$

where $C_{ip(a)}$ is the LCAO coefficient of the atomic orbital $\chi_{p(a)}$ centered on atom a. The above expression shows that the intensity σ_i is roughly proportional to the square of the modulus of the overlap between φ_i and Ψ_k. This observation is at the origin of the Gelius intensity model,[8] where σ_i is partitioned in atomic cross sections σ_{ia}, which are approximated by a weighted sum of partial atomic cross sections $\sigma_{ip(a)}$:

$$\sigma_i = \sum_a \sigma_{ia} \approx \sum_a \sum_{p(a)} P_{ip(a)} \sigma_{ia} \tag{6}$$

In (6) the $\sigma_{ip(a)}$ is the cross section of the atomic function $\chi_{p(a)}$ (1s, 2s, $2p_x$, etc.) of atom a and $P_{ip(a)}$ is either the gross atomic or the net atomic Mulliken population[9] of atomic function $\chi_{p(a)}$ in orbital i. The intensity J_i^{XPS} that we use in this work for the theoretical simulations of the valence region of XPS spectra is based on the net atomic Mulliken population version of (6); it has the following explicit form:

$$\sigma_i \approx J_i^{XPS} = \sum_a \sum_{p(a)} |C_{ip(a)}|^2 \sigma_{p(a)} \tag{7}$$

X-ray Emission Spectroscopy (XES).[10] For the presentation of XES we directly place ourselves in the context of the one-electron model. If the photoelectron is ejected from a core orbital φ_i^c, the resulting ion can relax in two different ways, as shown in Figure 1. The first, by far the dominant one for light elements, is the Auger process in which a second electron is ejected, leaving a doubly ionized atom. The second is the X-ray emission in which an electron from an outer occupied orbital φ_j fills in the core hole. The corresponding energy is, to a first approximation, equal to the difference between the one-electron energy levels ϵ_j and ϵ_i^c; thus, the emitted photon has the energy

$$E \approx \epsilon_j - \epsilon_i^c \tag{8}$$

In the one-electron approximation, the intensity τ_{ij} of the emitted signal is given by

$$\tau_{i,j} \propto |\int \varphi_i^c(\mathbf{r}) \, (e\mathbf{r}) \varphi_j(\mathbf{r}) \, d\tau|^2 \tag{9}$$

Since the wavelength emitted by oxygen (O Kα line), the element of interest to us in this work, is large (λ = 23.62 Å) relative to atomic dimensions, (9) is governed by selection rules, implying that the orbital angular momentum quantum number can only change under the constraint $\Delta l = \pm 1$. Thus transitions from outer occupied orbitals to s-type holes in a given atom can only arise from orbitals with p character on the same atom.

The polymer samples studied in this paper contain only hydrogen, carbon, and oxygen atoms, so the cores holes will be of the 1s type only and correspond to the atomic function $\chi_{1s(a)}$. Therefore the XES transition intensity can be written as

$$\tau_{1s(a),j} = N |\int \chi_{1s(a)}(e\mathbf{r}) \sum_a \sum_{p(a)} C_{jp(a)} \chi_{p(a)}(\mathbf{r}) \, d\tau|^2 \tag{10}$$

where N is a normalization factor.

Taking into account the above-mentioned selection rule and neglecting the terms involving orbital products on different atoms, an approximate intensity $J_{1s(a),j}^{XES}$ can be derived from (10)

$$\tau_{1s(a),j} \approx J_{1s(a),j}^{XES} = N' \sum_a |C_{j[2p(a)]l}|^2 \tag{11}$$

where N' is a normalization factor, which includes the units of atomic dipole intensities.

The fine structure observed in the valence band region of an X-ray photoelectron spectrum maps out, on an energy scale, the occupied molecular orbitals. The relative peak intensities are, however, governed by the sum of the ionization cross sections (σ_i) of each atomic orbital

participating in the formation of a molecular orbital multiplied by the fractional contribution it makes to the MO as explicitly written in (7). For X-ray emission spectra the situation is slightly different since an X-ray emission spectrum not only is element specific but also is subject to quite strict selection rules. Thus the fine structure observed in an oxygen Kα spectrum, for example, indicates, again on an energy scale, those molecular orbitals that have some O_{2p} character. The relative intensities are directly proportional to the fraction of 2p character present in each orbital. This is because the transition operator $\langle \chi_{1s(O)}|er|\chi_{2p(O)}\rangle$, in this case will be the same for each molecular orbital. The *absolute* determination of the coefficient $C_{j[2p(O)]}$ for each molecular orbital is much more difficult. Despite this limitation, X-ray emision spectra can provide a useful check upon theoretical predictions of molecular electronic structure. This is especially true when the X-ray emission spectrum is aligned by using experimental core level ionization energies with the X-ray photoelectron valence band spectrum, as some of the atomic orbital composition of the valence band molecular orbitals is then indicated directly.

This brief presentation of the XPS and XES spectroscopies emphasizes also the importance and necessity for their interpretation of having the support of theoretical calculations on model molecular systems of the materials investigated.

3. Theoretical Calculations and Model Molecules

Since the use of theoretical calculations in predicting and explaining features of the experimental XPS valence band spectra of polymers in connection with their primary and secondary structures has already been discussed,[3,11,12] we limit this section to the essential points of the calculations.

The calculations have been carried out at the ab initio level (STO-3G basis) using the GAUSSIAN 82 series of programs.[13] The requested convergence on density matrix was fixed to 10^{-8} and the integral cutoff was fixed equal to 10^{-10} hartee. The use of the minimal STO-3G basis is imposed by our limited computational facilitites and the size of the model oligomers used to simulate long polymer chains. The qualitative ordering of the STO-3G levels on the closely related model oligomers of poly(oxymethylene)[4] has been checked against experimental and more refined theoretical calculations. Thus, as in the case of the poly(oxymethylene) study, we expect reliable predicted qualitative trends for the systems considered in this work. In order to have a better comparison of theory with XPS and XES experimental data, all the ab inition one-electron energies ϵ_i are linearly contracted and shifted on the energy scale according to the relation

$$\epsilon_i' = 0.82\epsilon_i - 2.90 \qquad (12)$$

This empirical procedure is nothing but a pragmatic and convenient scaling of the theoretical data, which provides a better match with the experimental values. It essentially accounts for the deficiencies of basis set limitations. One generally observes that the larger the atomic basis sets, the closer to unity the slope of a linear regression between the one-electron energies and the experimental ionization energies is. This procedure does not cure the insufficiencies of the one-electron model and Koopmans' approximation mentioned in section 2. In the comparisons of theoretical and experimental spectra (section 5), the theoretical values to which we will refer will always correspond the scaled energies ϵ_i' defined in (12).

The validity of the Koopmans' theorem[7] in the interpretation of the XPS spectra is assumed, and the Gelius intensity model[8] is used in constructing the theoretical valence XPS spectra. They result from the addition of the theoretical intensity of the peaks centered at the corrected ab initio one-electron energy levels ϵ_i' of the occupied valence one-electron states. Each peak is represented by a linear combination of one Lorentzian and one Gaussian curve, each having the same weight and full-width at half-maximum (fwhm = 1.5 eV). The peak height is weighted according to the intensity J_i^{XPS} calculated from (7). The relative atomic photoionization cross sections used for O_{2s}, O_{2p}, C_{2s}, C_{2p}, and H_{1s} are 1.400, 0.159, 1.000, 0.077, and 0.000, respectively.

The intensity $J^{XES}_{1s(O),j}$ of oxygen XES spectral lines could be obtained from (11), i.e., by summing the square of the LCAO coefficients $|C_{j[2p(O)]}|^2$ of the atomic functions $\chi_{2p(O)l}$ centered on a given oxygen atom O; $l = x, y$, and z. Each peak in the theoretical XES spectra could also be represented by the same combination of Lorentzian–Gaussian curves as those for XPS spectra. In this work, however, we have not attempted to construct the theoretically simulated XES spectra of the model molecules because the presently limited resolution of the experimental setup on which measurements have been made precludes detailed comparisons with theoretical simulations.

The present state of our computational facilities limits the number of atomic orbitals that can be considered and imposes a compromise between the size of the model molecules and the desire for the best possible theoretical simulation of the valence band region of poly(ethylene oxide) and poly(vinyl alcohol). The model oligomers have to be long enough to yield stable shapes of the theoretical spectra.[4,11] Thus, the oligomers representing POE and PVOH, respectively, are $CH_3CH_2O(CH_2CH_2O)_4CH_2CH_3$ and $CH_3CH(OH)CH_2CH(OH)CH_3$. In the case of the diol molecule, the meso isomer has been chosen to mimic the polymer atacticity. The geometry of the model oligomers representing the polymers is also important because, as previously reported,[4,11,12] the molecular structure is often fingerprinted in the shape of the XPS valence band spectrum. Thus we represent the polymers by model molecules having the same geometry features as found or assumed for the polymeric material. As confirmed by infrared spectroscopy measurements on a cast solvent film, the conformation of the studied POE is planar zigzag;[14] thus, this geometrical feature has been imposed in the geometry of the model oligomer of POE. Mainly due to the interchain hydrogen bonds, the chain structure of the crystalline atactic PVOH is planar zigzag,[15] but no information is available on the HOCC torsional angle. Thus, a geometry optimization has been performed at the STO-3G level on the 2,4-pentanediol to obtain a sensible value for this missing geometrical parameter. The structures of the oligomers are presented in Figure 2, and the experimental molecular parameters (bond lengths, valence angles, torsional angles) of the corresponding polymers are listed in Table I. The values supplemented by theoretical calculations are marked with an asterisk and called optimized parameters in the table.

4. Experimental Section

Preparation of the Samples. The origin of the polymer samples and their main physicochemical characteristics are summarized in Table II. When the purity of the samples, checked on the basis of the ratio of the experimental peak intensities of the C_{1s} and O_{1s} core lines (I_C/I_O),[16] was not satisfactory, the polymers have been recrystallized just before use.

XPS Measurements. The photoelectron spectra were recorded with a Hewlett-Packard 5950A spectrometer using the

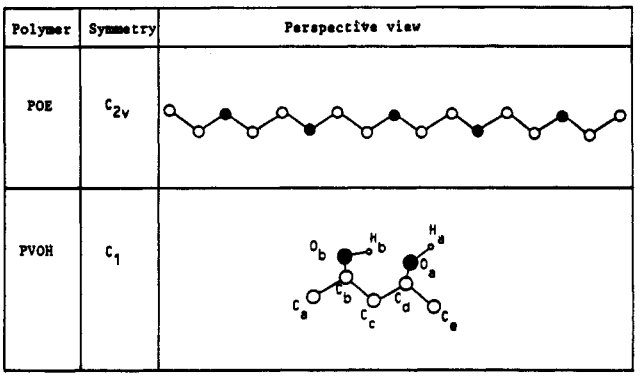

Figure 2. Symmetry group and perspective view of the molecules used to modelize the poly(ethylene oxide) (POE) and poly(vinyl alcohol) (PVOH).

Al Kα monochromatized radiation ($h\nu$ = 1486.6 eV). Films of the polymer samples, obtained from solvent casting, are deposited on a gold substrate and introduced in a vacuum chamber (pressure below 10^{-8} Torr). The temperature was fixed at 273 K by cooling with liquid nitrogen. During the analysis, the positive electrostatic surface charge (due to the photoelectrons ejection) of the insulating samples was kept constant by the use of an electron flood gun. The final experimental valence bands were obtained by adding up several recordings, each accumulated for 6 h.

The binding energy of the valence band lines is referenced to the C_{1s} peak of the other OCH_2- group of the samples. The C_{1s} peaks were themselves calibrated by mixing the polymer with poly(trifluoroethylene) for which the C_{1s} core energy levels, *C*F and *C*F_2, are fixed at 289.4 and 291.6 eV, respectively. The radiation damage at the surface, checked by monitoring the C_{1s} peak after the analysis, was minimized by cooling and operating with short accumulation periods.

XES Measurements. The powdered polymer samples were mounted by being pressed into a fine copper mesh, and their X-ray emission spectra were measured by a Philips PW 1410 spectrometer operated at about 10^{-1} Torr. The spectra were excited by irradiation, with the soft X-rays and low-energy electrons emitted by a CGR (Compagnie Générale de Radiation) Elent-10, open-window gas discharge tube (3 mA, 5 kV), and dispersed by a rubidium acid phthalate crystal ($2d$ = 26.12 Å).

The use of the "fine" collimator (150-μm blade separation) together with a small auxiliary collimator mounted at right angles to the main collimator to control "horizontal divergence" yielded oxygen Kα spectra with a minimum fwhm of about 2.6 eV. The X-rays were detected in a proportional counter fitted with a 1-μm Mylar window (flow gas, 90% Ar + 10% CH_4, 1 atm of pressure). The output pulses were amplified with Harwell 2000 electronics and counted on CBM PET microcomputers. These computers were also used for data storage, handling, and analysis. Spectra were collected digitally by multiple scanning over the range 125–135° 2θ (θ is the angle of the X-ray beam upon the diffracting crystal within the spectrometer). The resulting sum was smoothed by using polynomial techniques. About 15 min was required to collect the data for each X-ray emission spectrum shown in the figures. Spectra were calibrated by reference to the O Kα from quartz ($h\nu$ = 525.8 eV).

5. Results

Before comparison and discussion of the experimental data of the different samples, it is important to note that a complete interpretation would require information on the intramolecular relaxation[17,18] phenomenon involved in the photoelectronic process. In addition to the intramolecular relaxation energy, due to the redistribution of the positive charge along the chain, it is also necessary to consider the intermolecular relaxation energy, mostly because of the stabilization of the charge by polar interactions with the closest chains. For poly(ethylene), Pireaux et al.[19] give a value of 1.2 eV for the intermolecular relaxation energy. For the polar poly(vinyl alcohol),[20,21] the corresponding value is 1.1 eV and is close to that of poly(ethylene). It is thus reasonable to think that the intermolecular relaxation energy of poly(oxyethylene) is of the same order. Furthermore, in the comparison of experimental spectra and theoretical simulations, we assume that all valence levels are similarly affected by these relaxation phenomena.

A. Core Level Spectra. In this part, the experimental results on the XPS C_{1s} and O_{1s} core levels, respectively, parts a and b of Figure 3, of POE and PVOH are briefly discussed. It is immediately noticeable from these figures that the structure of the core level spectra is different for the two systems, thereby showing their dependence on structural isomerism.

As both monomeric units contain only one oxygen atom, there is only one core level line situated at 532.4 and 532.1 eV for POE and PVOH, respectively. The observed difference in binding energy is most probably due to the larger negative charges on the oxygen atoms involved in the C–*O*–H linkage compared to those in the ether function C–*O*–C. This can be related to a more efficient electron attractive effect of the oxygen atom in the C–*O*–H group than in C–O–H. Indeed, ab initio STO-3G calculations on the model molecules considered in this work predict that the atomic charge on the central oxygen in CH_3-$CH_2O(CH_2CH_2O)_4CH_2CH_3$ is −0.25|*e*|, while the oxygens O_b and O_a in $CH_3CH(O_bH)CH_2CH(O_aH)CH_3$ bear −0.35|*e*| and −0.30|*e*| charges. It is worth pointing out that, in the model compound of PVOH, O_bH is involved in a hydrogen bond with O_a, $O_bH...O_a$ (see also Figure 2), which is marked by this significant difference in the atomic charges of both oxygens, −0.35|*e*| and −0.30|*e*|, respectively. Poly(vinyl alcohol) is known[15] to have many interchain hydrogen bonds. Thus the difference is the observed O_{1s} binding energies for PVOH and POE reflects not only the difference between C–*O*–C and C–*O*–H bonds but also the existence of these hydrogen bonds.

As expected from the molecular structure of the monomeric units, the C_{1s} spectrum of poly(ethylene oxide) shows only one peak situated at 286.1 eV, while the C_{1s} core level spectrum of PVOH is composed of two well-resolved lines: the lowest C_{1s} binding energy peak at 284.5 eV is assigned to the methylene group $-CH_2-$; the other at 285.9 eV corresponds to the $-C(OH)H-$ moiety.

Thus the two compounds are easily distinguished on the basis of the core level spectra. Note also that both samples are free of contamination by hydrocarbons, and their purity is quite satisfactory since the atomic composition, calculated from the experimental intensity ratio of carbon C_{1s} to O_{1s} peaks, I_C/I_O, is 1.99 and 2.00 for POE and PVOH, respectively, while the theoretical value for both polymers is equal to 2.00.

B. Valence Level Spectra. To facilitate comparison, the experimental and theoretical XPS spectra as well as the corresponding experimental XES spectrum are presented in superimposition in Figures 4 and 6, respectively, for POE and PVOH. The structure observed in the high-energy region (E > 527 eV) of the O Kα spectra (XES) is due to diffracting crystal fluorescence and to transitions in multiple ionized states (Wentzel–Druyvesteyn satellites). As the purpose of the present study is to compare the valence contributions of XPS and XES, only the regions of lowest photon energies will be interpreted in detail and the structure at E > 527 eV of the XES spectra will not be considered.

I. Poly(ethylene oxide). The three spectra (XPS, XES, and theory) of poly(ethylene oxide) are shown in

Table I
Bond Lengths (Å), Valence Angles (deg), and Torsional Angles (deg) Used in the Model Molecules for the Poly(ethylene oxide) and Poly(vinyl alcohol)

polymer	conformn	model molecule	bond lengths, Å		valence angles, deg		torsional angles, deg	
POE	PZZ[11]	$CH_3CH_2O(CH_2CH_2O)_4CH_2CH_3$	C–C	1.54	C–C–O	109.47	C–C–O–C	180
			C–O	1.43	C–O–C	109.47	O–C–C–O	180
PVOH	PZZ[12]	$C_aH_3C_bH(O_aH_a)C_cH_2C_dH(O_bH_b)C_eH_3$	C_a–C_b	1.55	C_a–C_b–C_c	109.47	C_a–C_b–C_c–C_d	180
			C–O	1.4	H_a–O–C_b	105.94	H_a–O_a–C_b–C_c	68.5[a]
					C_a–C_d–O	109.47	H_b–O_b–C_d–C_c	38.9[a]

[a] Optimized parameters.

Table II
Origin, Molecular Weight (M_w), and Melting Point, T_m (°C), of the Studied Polymers

polymer	origin	M_w	T_m, °C
poly(vinyl alcohol)	Aldrich Co. cat. no. 18251-6	115 000	258
poly(ethylene oxide)	Union Carbide Polyox coagulant	5 000 000	65

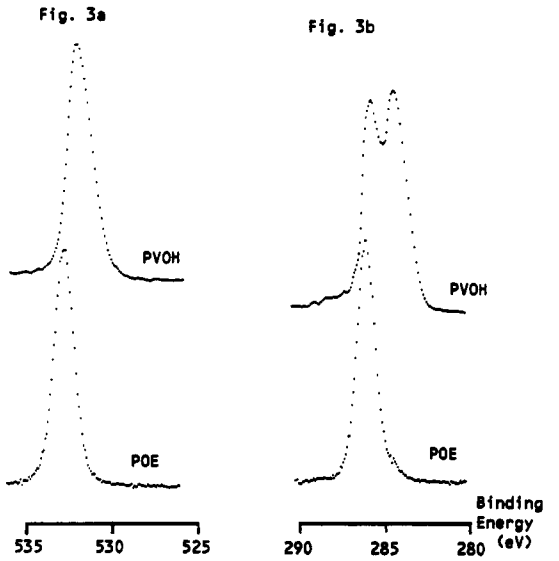

Figure 3. O_{1s} (a) and C_{1s} (b) core level spectra of the oxygen and carbon atoms in poly(ethylene oxide) and poly(vinyl alcohol).

Figure 4. Experimental and theoretical XPS valence band spectra are very similar, and the characteristics of the main peaks are summarized in Table III. Both in the experimental and theoretical XPS spectra, four regions can be distinguished on the energy scale. They are denoted A–D in the figure. This correspondence allows a characterization of the peaks in terms of the ab initio results on the model oligomer $CH_3CH_2O(CH_2CH_2O)_4CH_2CH_3$.

Peak A, around 26 eV, relates to molecular electronic levels where the O_{2s} atomic orbital contributions are dominant and the high intensity of the line is due to the large relative atomic photoionization cross section of O_{2s}; see section 3.

In region B, the three peaks B1, B2, and B3 located between 19 and 14 eV are mainly due to the contribution of the C_{2s} and O_{2s} atomic orbitals in the corresponding molecular levels. Peak B1 is attributed to the σ_{CC} bonding orbitals while peak B3 can be related to the σ_{CC} and σ_{CO} antibonding valence levels. The shape and structure, i.e., line positions and relative intensities, in that part of the theoretical and experimental spectra fit reasonably well; this is especially true for peaks B1 and B3. There is, however, a notable discrepancy between theory and experiment in the relative intensity of peak B2. In the experimental spectrum, the intensity of B2 is comparable to that of B1, while in the theoretical simulation it appears

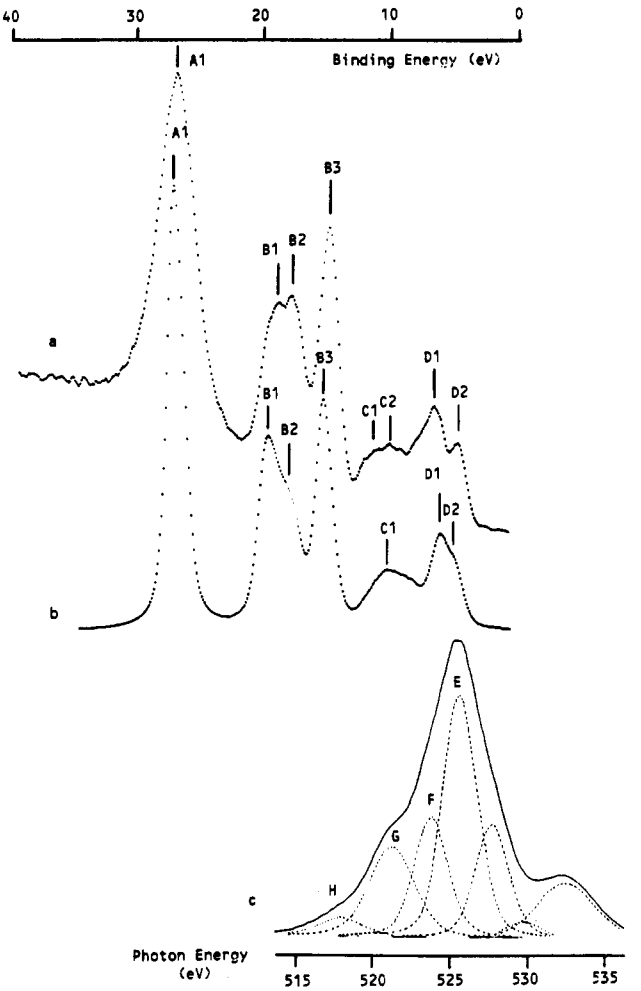

Figure 4. Experimental (a) and theoretically simulated (b) XPS valence band spectra of poly(ethylene oxide). O Kα X-ray emission spectrum (c) of poly(ethylene oxide).

Table III
Position (eV) of the Peaks Belonging to Theoretical and Experimental XPS Valence Band and XES Spectra of Poly(ethylene oxide)

peak label	XPS theory	XPS expt	peak label	XES: expt
A1	26.22 (35.43)	26.30		
B1	19.23 (26.92)	18.58		
B2	17.70 (25.02)	17.51		
B3	14.80 (21.50)	14.57	H	518.7
C1	9.25 (14.78)	11.35		
C2		9.49	G	521.3
D1	5.79 (10.58)	6.35	F	523.8
D2	4.83 (9.41)	4.49	E	525.7

mainly as a shoulder of the B1 peak. The origin of this difference is difficult to assess since already in the theoretical work several weaknesses could be invoked, among which the unrefined nature of the intensity model is probably the leading factor, but one cannot discard

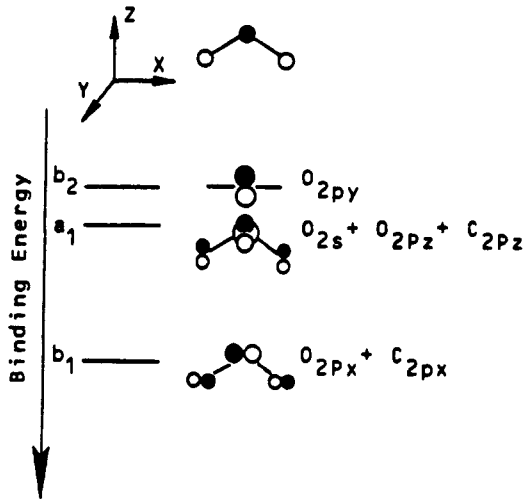

Figure 5. Schematic view of the formation of the highest binding energy molecular orbitals in the COC segment (XPS valence band region C and D).

effects due to the basis set limitation and the inadequacy of the Hartree–Fock and Koopmans' approximations. More rigorous theoretical treatments on smaller model molecules combined with suitable experiments would be necessary to sort out this problem.

Also very interesting, but difficult to interpret due to lower intensities, are the regions C and D in the XPS spectra. In the C region, the absence of a clearcut structure reflects the presence of many electronic states where mainly O_{2p} and many C_{2p} atomic orbitals participate. Nevertheless, it is possible to see two peaks, C1 and C2, located at 11.35 and 9.49 eV in the experimental spectrum. In the theoretical spectrum only the top of the band at 10 eV is to be considered; the nature of these structures will be discussed below in more detail using the ab initio results.

Finally, the D region shows two main peaks both in the theoretical and experimental spectra. The first one, D1, has a binding energy equal to 6.35 and 5.79 eV in the experimental and theoretical spectra, respectively. The second one, D2, is experimentally well-resolved at 4.49 eV, while in the theoretical spectrum it appears as a shoulder of D1 with a binding energy of 4.83 eV.

Exploiting the ab initio results on $CH_3CH_2O(CH_2CH_2O)_4CH_2CH_3$, the model molecule for POE, makes possible a more detailed interpretation of the valence XPS regions D and C. In the model molecule, the five highest occupied molecular orbitals include only C_{2p_y} and O_{2p_y} atomic orbitals (the $2p_y$ orbitals are perpendicular to the σ-plane containing the chain; see also Figure 5), thus leading to what could be called pseudo-π molecular orbitals. Furthermore, the weights of C_{2p_y} contributions are quite small (<20%) compared to those of O_{2p_y} in these five molecular orbitals, which thus could also be viewed as lone pairs on the oxygen atoms. The calculated energies of the five molecular orbitals lie in a narrow energy interval −4.68 to −4.58 eV so that they together form a well-distinct electronic band to which corresponds the well-resolved D2 peak in the experimental XPS spectrum.

The next seven electronic states below the ones just described are distributed on the energy scale over the interval (theoretical values) [−5.57 to −6.89 eV]. They correspond to molecular orbitals with σ_{CO} and σ_{CC} character. In the five molecular orbitals of lower binding energies, the weights of the O_{2p_z}, C_{2p_z}, and especially O_{2s} atomic orbitals are more important than C_{2p_z} and O_{2p_z}, which explains the higher intensity of peak D1 compared to that of peak D2. The present theoretical analysis is in agreement with the results of previous experimental works on shorter molecules than those considered here, but having nevertheless a similar chemical and molecular structure. For instance, with gas-phase UPS measurements, Kimura and his co-workers[22] assign the two oxygen atom lone pairs of the ethylene glycol dimethyl ether molecule to the peaks of lowest binding energy, respectively, at 9.78 and 10.06 eV (note that in gas phase the zeros of the energy scale and the relaxation phenomena are different from those of bulk).

The states in the interval −9.50 to −11.35 eV contribute to peaks C1 and C2. They have loose σ_{CO}, and σ_{CH} characters, which result from the combination of C_{2p}, O_{2p}, and H_{1s} atomic orbitals. Due to the low value of the relative atomic photoionization cross section of the contributing atomic orbitals and the large energy interval over which these levels are distributed, the resulting XPS spectrum in the C region is of relatively low intensity and without distinct features.

Although of somewhat lower resolution than the XPS spectrum, the XES spectrum still shows a structure that can be resolved into seven components as shown in Figure 4. Voigt functions[23] (assumed 80% Gaussian) of various widths were used in the deconvolution: widths were chosen to reproduce the experimental curve. The three peaks with energies above 527 eV are due to crystal fluorescence and transitions in doubly ionized oxygen, but the four lower energy peaks, centered at 525.7, 523.8, 521.3, and 518.0 eV, reflect oxygen 2p character in the molecular orbitals of the polymer. Although the alignment is not perfect, due to the limitation in resolution present in both XPS and XES spectra, it can be seen from Figure 4 that the three first XES peaks correspond to D2 (E), D1 (F), and C(G) XPS peaks. The latest peak at 518.0 eV is (H) coming from the O_{2p} contribution to the molecular orbital having a large C_{2s} atomic character B3. The relative intensities of the O Kα X-ray emission peaks can be related directly to the relative amounts of O_{2p} character present in the different molecular orbitals. The peak at 525.7 eV being the most intense feature confirms the identification of D2 as being principally due to "lone pair" orbitals on oxygen. The distribution of O_{2p} character in the other molecular orbitals can be determined by ab initio calculations and approached in a more direct way by reference to the following three atomic models (Figure 5). The local symmetry at each oxygen, C–*O*–C, corresponds to the point group C_{2v}, so that the three O_{2p} orbitals will transfiorm as $2p_x$, (b_1), $2p_y$ (b_2), and $2p_z$ (a_1).

The least tightly bound orbital at any oxygen will therefore correspond to the $2p_y$ (b_2), a lone pair. The other two orbitals will participate in bond formation with carbon generating orbitals of a_1 and b_1 character. In the simplest case, if the C–O–C angle is greater than 90°, then the b_1 orbital will be the more tightly bound but with less O_{2p} character than the a_1 orbital, which will be less tightly bound but with more O_{2p} character. As the C–O–C angle opens from 90° to 180°, the divergence in b_1 and a_1 energies will increase, with the a_1 orbital approaching the energy of the b_2 orbital. In more complicated molecules (such as $CH_3CH_2O(CH_2CH_2O)_4CH_2CH_3$) each orbital will be split into many, forming bands, but the general features should be retained as seen before.

The O Kα emission spectrum suggested by this simple model for molecules with the C–O–C angles greater than 90° should show three features: a weak peak at low X-ray energy (b_1), a much more intense peak close to the main peak (a_1), and, somewhat more intense, the main peak

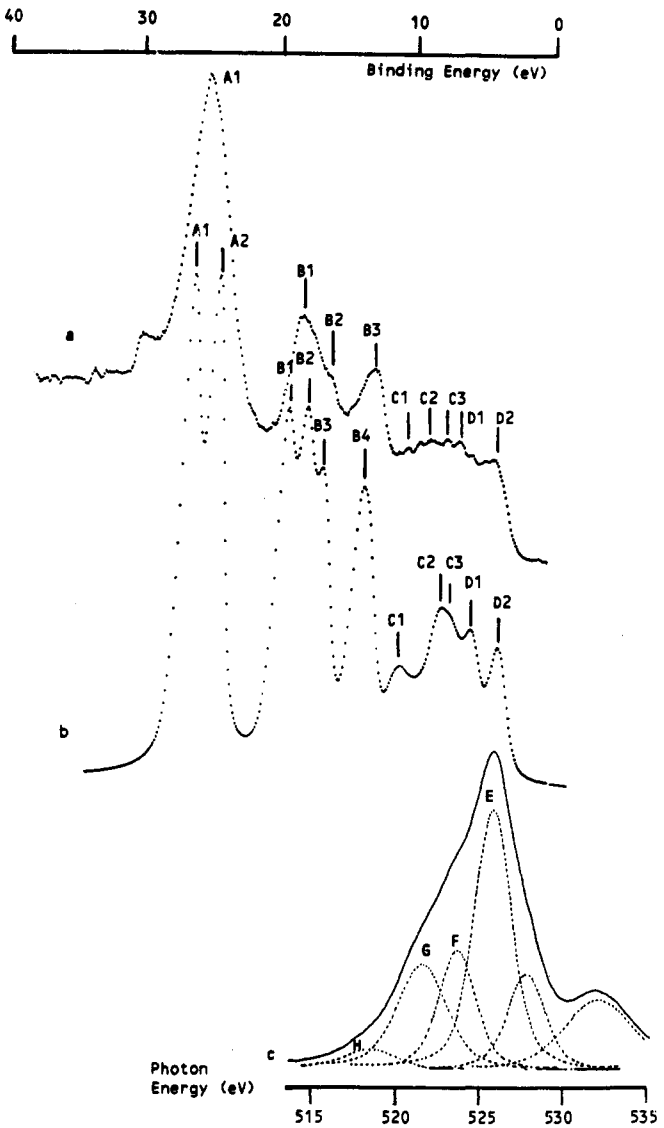

Figure 6. Experimental (a) and theoretically simulated (b) XPS valence band spectra of poly(vinyl alcohol). O Kα X-ray emission spectrum (c) of poly(vinyl alcohol).

itself (b_2) (see Figure 5).

II. Poly(vinyl alcohol). Changing the molecular structure of POE into PVOH modifies the relative positions of the atoms. Our previous results[1-4,11,12] have shown that such structural differences can also modify the distribution of the molecular electronic levels to such an extent that it can be observed in the valence XPS spectra. In the following we analyze the shape of the valence XPS and XES spectra of PVOH, compare it with the results on POE just discussed, and attempt to relate the differences to structural isomerism on the basis of the theoretical results on the model molecules.

The theoretical and experimental XPS spectra and the XES experimental spectrum of PVOH are presented in Figure 6. As was already the case for POE, both experimental and theoretical XPS spectra of PVOH are divided into four regions and the parameters of their corresponding peaks are summarized in Table IV.

In the experimental spectrum there is a single peak A1 at a binding energy value of 25.65 eV corresponding to molecular levels where the O_{2s} atomic orbital contributions are very important. Compared to the same peak in the POE XPS valence band spectrum, there is not much difference, except that in POE it appears at 26.30 eV and it is slightly narrower. In the theoretical spectrum, on the

Table IV
Position (eV) of the Peaks Belonging to Theoretical and Experimental XPS Valence Band and XES Spectra of Poly(vinyl alcohol)

peak label	XPS theory	XPS expt	peak label	XES: expt
A1	26.98 (36.35)	25.65		
A2	25.06 (34.01)			
B1	19.98 (27.84)	18.85		
B2	18.54 (26.08)	17.12		
B3	17.17 (24.42)	13.27		
B4	14.20 (20.80)		H	518.4
C1	11.46 (17.47)	11.00		
C2	8.57 (13.95)	9.00	G	520.8
C3	7.71 (12.91)	8.13		
D1	6.15 (11.01)	7.12	F	523.5
D2	4.22 (8.66)	4.56	E	525.8

contrary, there are two well-resolved lines, A1 and A2, which result from the different bonding situation of O_b and O_a in the model molecule (Figure 2) and show the sensitivity of the deep valence levels to bonding. In the actual polymer, however, inter- and intrachain hydrogen bonds can coexist and, due to local differences in the chain structure leading to steric hindrances, these bonds will have varying strengths. The net effect is statistical and yields a less structured peak in the experimental case. Thus, $CH_3CH(O_bH)CH_2CH(O_aH)CH_3$, the theoretical model molecule of PVOH, only describes two extreme situations. From a pragmatic point of view and ignoring configurational isomerism as well as intermolecular interactions, a peak around 26 eV in the experimental XPS valence spectra can be considered as a signature of valence 2s levels of singly bonded oxygen atoms to carbon and (or) hydrogen atoms.

In the binding energy interval, 20 to 12 eV, are the molecular levels with important O_{2s} and particularly C_{2s} atomic orbital participations. Both theory and experiment show that these states are grouped into two bands centered at 18 eV (bonding) and 13 eV (mostly antibonding) on the binding energy scale. A closer examination of these spectra reveals minor discrepancies between experience and theory. In the experimental spectrum, the band of largest binding energy is composed of two peaks, B1 (18.85 eV) and B2 (17.12 eV), the latter being mainly a shoulder of B1, and the antibonding structure shows only one distinct line B3 at 13.27 eV. The bonding part of the B region in the theoretical spectrum is composed of three peaks B1 (19.98 eV), B2 (18.54 eV), and B3 (17.17 eV), which correspond to the experimental B1 and B2 lines. The antibonding part has one line B4 at 14.20 eV.

Comparison between regions B of theoretical and experimental spectra does not provide a fully satisfactory agreement. Three distinct peaks B1, B2, and B3 form the bonding band in the stimulated spectrum instead of two in the experiment. This is most likely to a somewhat small fwhm value (1.5 eV) of the convolution function used. Moreover, their theoretical intensities, normalized with respect to the O_{2s} one, are higher than the experimental ones.

When the results on PVOH are compared with those previously obtained for POE, important spectral modifications are to be pointed out. The first concerns the relative intensity of the bonding and antibonding parts in the B region. In the POE valence band spectrum, the sharp peak (B3) at 14.57 eV has a much higher intensity than the bonding one (B1 + B2) at 18 eV. The opposite is found for PVOH; the antibonding structure is more spread and of lower relative intensity than that in POE.

Attempts are now being made to explain the differences between regions B in XPS experimental spectra of POE

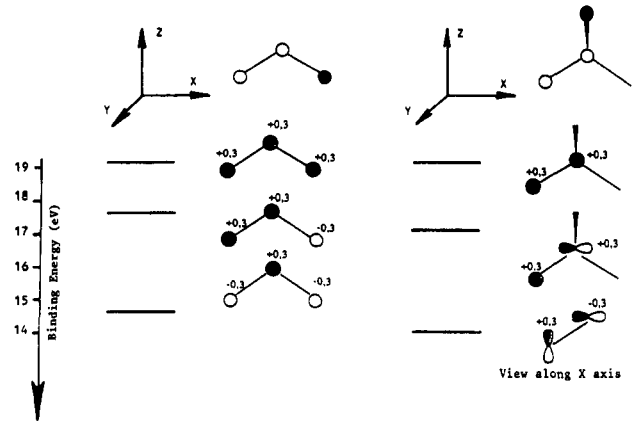

Figure 7. Schematic view of the formation of molecular orbitals, corresponding to XPS valence band region B, in the CCO segment of poly(ethylene oxide) and poly(vinyl alcohol).

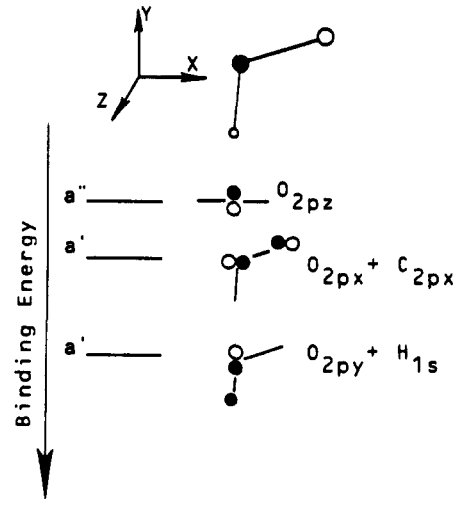

Figure 8. Schematic view of the formation of the highest binding energy molecular orbitals in the HOC segment.

and PVOH in terms of the configurational effect. To this end, we transpose the ab initio (STO-3G level) results on model molecules to the construction of the molecular levels in this region in the monomeric units chosen as the simplest reference model (Figure 7).

In both systems, the two first molecular levels are characterized by the bonding interaction between the carbon atoms, with a significant amount of C_{2p} participation in PVOH unit. In POE and PVOH, the less stable level comes from the out of phase combination of O_{2s} and C_{2s} atomic orbitals (not represented in Figure 7 for the PVOH unit). Moreover, bonding interactions between C_{2p} and O_{2p} atomic orbitals decrease the monoelectronic energy of this level in PVOH.

When the size of the molecule increases, the numerous molecular levels are grouped in bands whose energy widths are centered on the binding energies of these three previously described monoelectronic levels. So, these bands can be experimentally identified as the three XPS valence band structures B1, B2, and B3 clearly evidenced for the two polymers POE and PVOH. This model also supplies quantitative information and shows that the low intensity of the B2 and B3 peaks in PVOH comes from the low cross section of the 2p atomic orbitals involved in the building of the molecular levels in this energy region.

This XP spectrum in the C–D region is characterized by a poor signal-to-noise ratio, which indicates that the corresponding orbitals are mostly O_{2p} and C_{2p} in character. This is confirmed (at least for oxygen) by the alignment of the O Kα XE spectrum, which shows that D2 together with D1, C3, and C2 represents molecular orbitals rich in O_{2p}. To gain some insight into the bonding in the region of the oxygen atom in the polymer, the COH group was used as a model. In this isolated system (point group C_s; Figure 8) the O_{2p_z} does not participate in the bonding and so generates a "lone pair" where the least tightly bound electrons reside (HOMO). O_{2p_x} and O_{2p_y} form C–O and O–H bonds with increasing ionization energies. This ordering is confirmed by more sophisticated calculations (6-31G ab initio) for small molecules such as methanol (it is noted that the presence of O_{2s} from these orbitals is not precluded). When this COH group is present in a polymer, the individual molecular orbitals will be broadened into bands but their essential nature will not be altered. Thus, it is possible to identify peak E (525.8 eV, O Kα; Figure 6) and D2 (4.46 eV, XP theory; Figure 6) as being due to a band of orbitals almost completely localized on the oxygen atoms. The XE peaks F and G can then be associated with molecular orbitals principally concerned with the σ bonding of oxygen to carbon and to hydrogen, peaks D1 (7.12 eV) and C2 (9.00 eV) (the intensities of these XP peaks can be rationalized as due to the admixture of a little O_{2s} character). The weak peak H, which aligns with the strong XP peaks B4 (theory) and B3 (XP experimental), confirms the presence of some O_{2p} character in this band, as required by the calculations for the PVOH model above.

Some subtle differences between POE and PVOH spectra in the 6–12-eV binding energy range can be discerned, which can probably be attributed to configurational changes in the monomeric units. More distinct features can be seen, for example, in the C region of POE than is that of PVOH. This can be rationalized as due to a greater localization of the σ_{CO} in POE and to broader, more dispersed bands of orbitals in PVOH. These changes are also reflected in the widths of the G and F peaks of the O Kα spectra, 2.62 eV (PVOH) and 2.55 eV (POE). G and F overlap more in PVOH, giving rise to a less structured O Kα peak than that for POE.

6. Conclusions

Modifications of the configuration of oxygenated polymers having a simple oxygenated function in their monomeric units (PVOH and POE) introduce changes in their valence level electronic structure. With the help of theoretical calculations on well-chosen model molecules, the interpretation of XPS and XES spectra is greatly facilitated. While the greatest effects of configurational changes are located in region B of the XPS spectra (20 to 14 eV), significant effects are also observed in region C, which corresponds to the least tightly bound valence band levels. Comparison with the oxygen Kα XE spectra shows these orbitals to be predominantly oxygen 2p in character. It is clear that to take full advantage of the potential of the XES method, it will be necessary to improve both resolution and the signal-to-noise ratio. So measurements on identical oxygenated systems using an improved XE spectrometer[24] would be most welcome in order to determine more accurately the modifications in electronic structure wrought by changes in polymer configuration. In addition, the experimental XES study on smaller molecules in the solid state should supply information on the role of band formation in the electronic structure of the polymer compared to that of the discrete monoelectronic level in gaseous molecules.

Acknowledgment. We are very grateful to the Science EEC Program for providing support (Project SC1-0016-

C) to the collaboration between the Queen Mary College in London, the University of Durham, and the Facultés Universitaires Notre-Dame de la Paix de Namur (FUNDP). They also thank the Belgian National Fund for Scientific Research, IBM-Belgium, and FUNDP for the use of the Namur Scientific Computing Facility, together with the Royal Society, the Science and Engineering Research Council (U.K.), and the Central Research Fund of London University for grants for the purchase of equipment.

References and Notes

(1) Delhalle, J.; André, J. M.; Delhalle, S.; Pireaux, J. J.; Caudano, R.; Verbist, J. J. *J. Chem. Phys.* **1974**, *60*, 595.
(2) Delhalle, J.; Montigny, R.; Demanet, C.; André, J. M. *Theor. Chim. Acta* **1979**, *50*, 343.
(3) Pireaux, J. J.; Riga, J.; Caudano, R.; Verbist, J. J. *ACS Symp. Ser.* **1981**, *No. 162*, 169.
(4) Boulanger, P.; Riga, J.; Verbist, J. J.; Delhalle, J. *Macromolecules* **1989**, *22*, 173.
(5) Policarpo, A. J. P.; Alves, M.; Dos Soutos, M.; Carvalho, M. *Nucl. Instrum.* **1972**, *102*, 337.
(6) Wendin, G. Photoelectron Spectra. *Structure and Bonding*; Springer-Verlag: Berlin, 1981; Vol. 45.
(7) Koopmans, T. A. *Physica* **1933**, *1*, 104.
(8) Gelius, U. *J. Electron Spectrosc. Relat. Phenom.* **1974**, *5*, 985.
(9) (A) Mulliken, R. S. *Rev. Mod. Phys.* **1951**, *4*, 1. (b) Mulliken, R. S. *Phys. Rev.* **1939**, *50*, 1029.
(10) Urch, D. S. In X-Ray Spectroscopy and Chemical Bonding in Minerals. *Chemical Bonding and Spectroscopy in Mineral Chemistry*; Berry, F. J., Vaughan, D. J., Eds.; Chapman and Hall: London, 1985; p 30.
(11) Boulanger, P.; Lazzaroni, R.; Verbist, J. J.; Delhalle, J. *Chem. Phys. Lett.* **1986**, *129*, 275.
(12) Delhalle, J.; Delhalle, S.; Riga, J. *J. Chem. Soc., Faraday Trans. 2* **1987**, 83.
(13) Binkley, J. S.; Frisch, M. J.; De Frees, D. J.; Raghavachari, K.; Whiteside, R. A.; Schelgel, M. B.; Fluder, E. M.; Pople, J. A. *GAUSSIAN82*; Carnegi-Mellon University: Pittsburgh, PA, 1982; implemented for the IBM 9377 by J. G. Fripiat.
(14) Ramana-Rao, G.; Castiglioni, C.; Gussoni, M.; Zerbi, G.; Martuscelli, E. *Polymer* **1985**, *26*, 811.
(15) Bunn, C. W. *Nature* **1984**, *161*, 929.
(16) The relative atomic content C/O is obtained from the relation: $C/O = I_C/I_{Of}$ where I_C and I_O are the measured intensities of the C_{1s} and O_{1s} core level peaks and f is an empirical factor determined from identical measurements on oxygenated hydrocarbons having a well-defined stoichiometry ($f = 2.63$).
(17) Duke, C. B. *Mol. Cryst. Liq. Cryst.* **1979**, *50*, 63.
(18) Salaneck, W. R. *CRC Crit. Rev. Solid State Mater. Sci.* **1985**, *12*, 267.
(19) Pireaux, J. J.; Caudano, R.; Svensson, S.; Basilier, E.; Malmqvist, P.-A.; Gelius, U.; Siegbahn, K. *J. Phys. (Paris)* **1977**, *38*, 1213; **1977**, 38, 1221.
(20) Seki, K.; Karlson, U. O.; Engelhardt, R.; Koch, E. E.; Schmidt, W. *Chem. Phys.* **1984**, *91*, 459.
(21) Xian, C. S.; Seki, K.; Inokuchi, H.; Hashimoto, S.; Ueno, N.; Sugita, K. *Bull. Chem. Soc. Jpn.* **1985**, *58*, 890.
(22) Kimura, K.; Katsumata, S.; Achiba, Y.; Yamasaki, T.; Iwata, S. *Handbook, of HeI Photoelectron Spectra of Fundamental Organic Molecules*; Japan Scientific Societies Press: Tokyo, 1981.
(23) Biggers, R. E.; Bell, J. T. *J. Mol. Spectrosc.* **1965**, *18*, 247.
(24) Rubensson, J.-E.; Wassdahl, N.; Brammer, R.; Nordgren, J. *J. Electron. Spectrosc. Relat. Phenom.* **1988**, *47*, 131.

Registry No. POE, 25322-68-3; PVOH, 9002-89-5.